

Are your **MRI contrast agents** cost-effective?

Learn more about generic **Gadolinium-Based Contrast Agents**.



**FRESENIUS  
KABI**

caring for life

**AJNR**

**Postoperative MRI Evaluation of a  
Radiofrequency Cordotomy Lesion for  
Intractable Cancer Pain**

A. Vedantam, P. Hou, T.L. Chi, K.R Hess, P.M. Dougherty,  
E. Bruera and A. Viswanathan

This information is current as  
of April 20, 2024.

*AJNR Am J Neuroradiol* published online 16 February 2017  
<http://www.ajnr.org/content/early/2017/02/16/ajnr.A5100>

# Postoperative MRI Evaluation of a Radiofrequency Cordotomy Lesion for Intractable Cancer Pain

 A. Vedantam,  P. Hou,  T.L. Chi,  K.R. Hess,  P.M. Dougherty,  E. Bruera, and  A. Viswanathan

## ABSTRACT

**BACKGROUND AND PURPOSE:** There are limited data on the use of postoperative imaging to evaluate the cordotomy lesion. We aimed to describe the cordotomy lesion by using postoperative MR imaging in patients after percutaneous cordotomy for intractable cancer pain.

**MATERIALS AND METHODS:** Postoperative MR imaging and clinical outcomes were prospectively obtained for 10 patients after percutaneous cordotomy for intractable cancer pain. Area, signal intensity, and location of the lesion were recorded. Clinical outcomes were measured by using the Visual Analog Scale and the Brief Pain Inventory–Short Form, and correlations with MR imaging metrics were evaluated.

**RESULTS:** Ten patients (5 men, 5 women; mean age,  $58.5 \pm 9.6$  years) were included in this study. The cordotomy lesion was hyperintense with central hypointense foci on T2-weighted MR imaging, and it was centered in the anterolateral quadrant at the C1–C2 level. The mean percentage of total cord area lesioned was  $24.9\% \pm 7.9\%$ , and most lesions were centered in the dorsolateral region of the anterolateral quadrant (66% of the anterolateral quadrant). The number of pial penetrations correlated with the percentage of total cord area that was lesioned ( $r = 0.78$ ; 95% CI, 0.44–0.89;  $P = .008$ ) and the length of T2-weighted hyperintensity ( $r = 0.85$ ; 95% CI, 0.54–0.89;  $P = .002$ ). No significant correlations were found between early clinical outcomes and quantitative MR imaging metrics.

**CONCLUSIONS:** We describe qualitative and quantitative characteristics of a cordotomy lesion on early postoperative MR imaging. The size and length of the lesion on MR imaging correlate with the number of pial penetrations. Larger studies are needed to further investigate the clinical correlates of MR imaging metrics after percutaneous cordotomy.

**ABBREVIATIONS:** ALQ = anterolateral quadrant; PIS = pain intensity score; PSS = pain severity score; VAS = Visual Analog Scale

Cordotomy is a lesion of the spinothalamic tract used to treat medically refractory pain. Percutaneous cordotomy is most commonly performed in the upper cervical spine at the C1–C2 level and targets the anterior and lateral spinothalamic tracts, which ascend in the anterolateral spinal cord.<sup>1</sup> This percutaneous technique, with either fluoroscopic guidance or an intraprocedural CT scan, has become the preferred method for performing

cordotomy because it requires minimal recovery time and can be performed during cancer treatment or at advanced stages of disease.<sup>2,3</sup>

Although cordotomy leads to effective pain relief in most patients,<sup>4</sup> up to 20% of patients may experience only partial or transient pain relief. These cordotomy failures may be due to incomplete ablation of the spinothalamic tract.<sup>5</sup> At present, there are limited data on the evaluation of patients with poor outcomes after percutaneous cordotomy. Prior research has shown great variability in the size of a radiofrequency lesion despite the same current flow<sup>6</sup>; however, the role of postoperative MR imaging to characterize the cordotomy lesion has not been explored thus far. Postoperative MR imaging of the cervical spinal cord can visualize the location and size of the lesion and may explain poor clinical outcome after cordotomy.

The present study aimed to describe the characteristics and clinical correlates of the cordotomy lesion by using postoperative MR imaging in a series of patients who underwent percutaneous cordotomy for intractable cancer pain.

Received September 29, 2016; accepted after revision December 9.

From the Department of Neurosurgery (A. Vedantam, A. Viswanathan), Baylor College of Medicine, Houston, Texas; and Departments of Imaging Physics (P.H.), Diagnostic Radiology (T.L.C.), Biostatistics (K.R.H.), Pain Medicine (P.M.D.), and Palliative Care and Rehabilitation Medicine (E.B.), University of Texas MD Anderson Cancer Center, Houston, Texas.

This work was supported by the American Cancer Society grant No. PEP-14-205-01.

Please address correspondence to Ashwin Viswanathan, MD, Department of Neurosurgery, Baylor College of Medicine, 7200 Cambridge, Suite 9A, MS: BCM650, Houston, TX 77030; e-mail: ashwinv@ubcm.edu

<http://dx.doi.org/10.3174/ajnr.A5100>

## MATERIALS AND METHODS

We conducted a prospective study at the University of Texas MD Anderson Cancer Center, Houston, Texas, for patients with unilateral intractable cancer-related pain below the C5 dermatome with a pain intensity  $\geq 4$  of 10. These patients are part of a randomized controlled trial, the results of which will be published separately. All patients underwent a percutaneous CT-guided cordotomy by the senior author after a detailed preoperative evaluation. All patients provided informed consent, and the study was approved by the institutional review board.

### Clinical Evaluation

Preoperative evaluation of pain was assessed with the Visual Analog Scale (VAS) score (from 0, no pain, to 10, worst pain) and the Brief Pain Inventory–Short Form. Postoperative pain was assessed by using the VAS and Brief Pain Inventory–Short Form on day 7 after the cordotomy. The VAS score represents the average pain experienced by the patient during the previous 24 hours. The Brief Pain Inventory–Short Form is a validated and responsive tool to measure pain outcomes for patients with cancer pain.<sup>7,8</sup> For the present study, the pain severity score (PSS) of the Brief Pain Inventory–Short Form (average score for questions 3–6)<sup>9</sup> and the pain intensity score (PIS) (average score for questions 9a–g) were used for analysis.

### Surgical Technique

A radiofrequency ablation technique (G4 radiofrequency generator and LCED disposable cordotomy electrode; Cosman Medical, Burlington, Massachusetts) was used to perform the cordotomies. Intravenous opioids, benzodiazepines, and either propofol or dexmedetomidine were used for patient comfort. A myelogram was performed before the procedure for most patients. Using intraprocedural CT guidance, we performed the cordotomy at the C1–C2 level.

As the spinal needle was advanced into the anterolateral quadrant (ALQ) of the spinal cord, multiple, limited, short-segment axial CT scans were obtained (Fig 1). The radiofrequency electrode with an exposed tip of 2 mm and a diameter of 0.2 mm was introduced into the spinal cord parenchyma. Intraoperative testing was then performed once the patient was fully awake and conversant. We ensured that motor stimulation (2 Hz, 100- $\mu$ s pulse width) did not elicit contractions below 1 V, thereby verifying a safe distance from the corticospinal tracts. We confirmed physiologic presence within the spinothalamic tract when sensory stimulation (100 Hz, 100  $\mu$ s) elicited contralateral paresthesias (optimally in the area of pain), at a voltage less than 0.2 V.

Two-to-4 radiofrequency ablations at 70°C–80°C were performed to lesion the spinothalamic tract. Clinical testing to assess the development of hypesthesia in the region of pain was performed between ablations. Further ablations were performed if hypesthesia was not present by clinical examination or if there was no elevation in the threshold for sensory stimulation. The number of pial penetrations and ablations performed was recorded for each patient. The number of pial penetrations exceeded the number of ablations when a given pial penetration did not elicit spinothalamic tract stimulation or if it led to unwanted corticospinal tract stimulation.

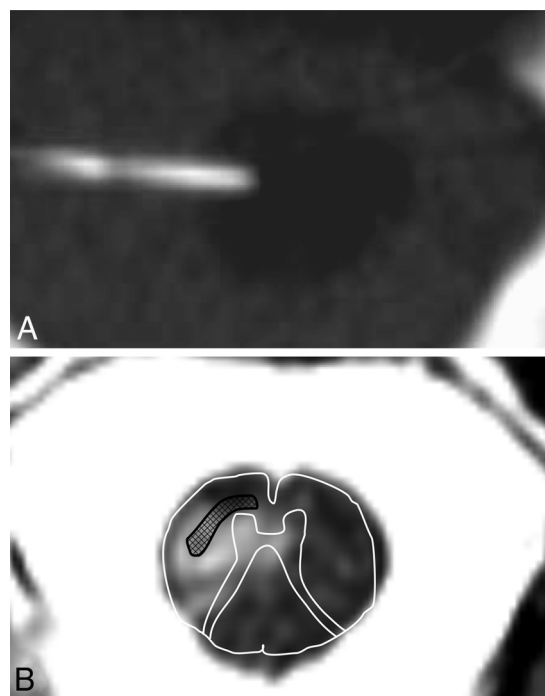


**FIG 1.** A, Intraprocedural CT myelogram showing the electrode entering the spinal cord parenchyma in the right anterolateral quadrant. B, Postoperative axial T2-weighted MR image of the cordotomy lesion with overlay of the cord anatomy and anatomic location of the anterolateral spinothalamic tracts marked (*black pattern*).

### Imaging

MR imaging of the cervical spine was performed on postoperative day 1. Sagittal and axial T1-weighted, T2-weighted, and contrast-enhanced images were obtained of the cervical spine on a Discovery wide-bore 750W 3T MR imaging scanner (GE Healthcare, Milwaukee, Wisconsin) with a maximum 3.3-g/cm gradient with a cervical spine and neck coil.

For sagittal images, we used a fast spin-echo technique: FOV = 200 mm, matrix = 352  $\times$  256, 4 averages, section thickness = 2.5 mm, gap = 0.3 mm, TR/TE = 4000/110 ms, TR/TE = 650/9 ms for T2- and T1-weighted imaging, respectively. For axial images, we used FSE: FOV = 160–180 mm, matrix = 320  $\times$  256, 4 averages, section thickness = 3.0 mm with a 0.3-mm gap, TR/TE = 4000/110 ms, TR/TE = 650/9 ms for T2- and T1-weighted imaging, respectively. Postcontrast, axial, and sagittal T1 images were obtained with the same acquisition parameters as for precontrast images. Acquisition time was between 4 and 5 minutes, depending on the number of sections covered.

Imaging analysis was performed off-line on OsiriX Imaging Software, V3.3 (<http://www.osirix-viewer.com>) after importing the DICOM images. Measurement of the lesion area and signal intensity was performed on axial T2-weighted images. The area of T2-hyperintensity was marked by using manual ROIs. The entire cord was divided into 4 quadrants as shown in Fig 2, and the area in the anterolateral and posterolateral quadrants was measured. The ALQ was further bisected to determine the proportion of the lesion in the anteromedial-versus-dorsolateral region. The length of the lesion was measured on sagittal T2-weighted images. Qualitative characteristics of the lesion on T1-weighted and contrast-enhanced scans were also recorded.

### Statistical Analysis

Statistical analysis was performed by using SPSS 20.0 (IBM, Armonk, New York). Descriptive statistics were used to report clinical outcome and quantitative MR imaging metrics. Correlations between MR imaging metrics, VAS scores, and Brief Pain Inventory–Short Form were performed by using the Spearman correlation. The association between enhancing lesions and the number of pial penetrations and lesions was studied by using the Fisher exact test. Means  $\pm$  SDs were reported, and the level of significance was set at  $P < .05$ .

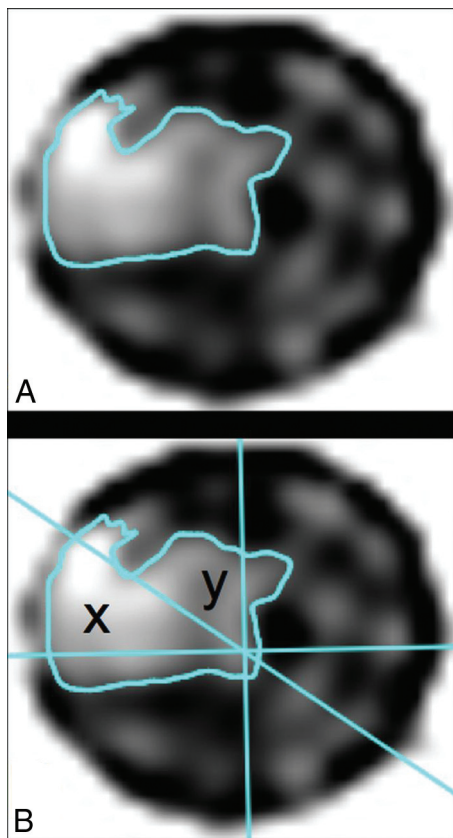


**FIG 2.** A, Axial T2-weighted image at the level of the cordotomy lesion for patient 1 shows the demarcated hyperintense lesion in the right anterolateral quadrant. B, Midline reference lines and the line bisecting the anterolateral quadrant show the portion of lesion in the dorsolateral (x) and ventromedial (y) regions of the anterolateral quadrant.

### RESULTS

We studied 10 consecutive patients (5 men, 5 women; mean age,  $58.5 \pm 9.6$  years) who underwent percutaneous cordotomy for intractable cancer pain (Table). There was a significant improvement in the VAS ( $5.5 \pm 2.7$ ,  $P < .001$ ), PSS ( $4.8 \pm 2.2$ ,  $P < .001$ ), and PIS scores ( $6.5 \pm 1.9$ ,  $P < .001$ ) on postoperative day 7 compared with the preoperative scores. All patients showed improvement in VAS, PIS, and PSS scores on postoperative day 7. Of the 10 patients included in this study, 8 patients had a VAS pain score of 0 or 1 on postoperative day 7. Two patients showed improvement in their VAS pain scores but had pain scores of  $>1$  on postoperative day 7 after cordotomy. All patients had an improvement in PSS and PIS scores, with most patients (PSS, 60%; PIS, 70%) having a score of zero on postoperative day 7. Five patients underwent 3 radiofrequency ablations, 4 patients underwent 2 ablations, and 1 patient underwent 4 ablations.

### Imaging Findings

The median time between cordotomy and MR imaging was 25.6 hours (range, 7.6–28.9 hours).

### Qualitative Data

All lesions were hyperintense with central hypointense foci on T2-weighted images and were centered in the anterolateral quadrant at the C1–C2 level (Figs 3 and 4). On T1-weighted imaging, the lesion was isointense in 9 patients and hyperintense in 1 patient. Five patients had contrast enhancement of the lesion, and 4 patients did not have contrast enhancement of the lesion. One patient did not undergo contrast-enhanced imaging due to an inability to lie still for this sequence. There was no significant difference in the median time interval between cordotomy and MR imaging between patients with enhancing cordotomy lesions and those without enhancing lesions (25.2 versus 25.6 hours,  $P = 1.0$ ; Mann-Whitney  $U$  test). There was no significant association between contrast enhancement and the number of lesions ( $P = 1.0$ ) and the number of pial penetrations ( $P = .52$ ).

### Quantitative Data

The mean lesion area was  $0.22 \pm 0.1$  cm<sup>2</sup>, and the mean percentage of total cord area that was lesioned was  $24.9\% \pm 7.9\%$ . The mean signal intensity of the lesions was  $798.7 \pm 272.2$ . The mean length of the T2-weighted hyperintensity on sagittal imaging was  $1.6 \pm 0.6$  cm. The mean percentage of lesions in the anterolateral quadrant was  $59.3\% \pm 13.4\%$ . Most lesions were centered in the

### Demographic and imaging data on 10 patients who underwent percutaneous cordotomy for intractable cancer pain

No.	Age (yr)	Sex	No. of Pial Penetrations	No. of RF Ablations	Area of T2W Lesion (cm <sup>2</sup> )	Area of T2W Lesion in ALQ (cm <sup>2</sup> )	Length of T2W Lesion (cm)
1	43	M	3	2	.1460	.0800	1.9850
2	66	F	3	3	.1880	.1150	1.7800
3	54	F	2	2	.1360	.0870	1.1950
4	53	F	2	3	.1170	.0850	.5480
5	76	M	3	3	.2980	.1670	2.3600
6	68	M	2	3	.2350	.1410	1.7450
7	61	M	3	2	.2460	.0710	1.8200
8	55	F	3	3	.2380	.1470	1.9000
9	59	F	2	4	.1330	.1060	.8200
10	50	M	3	2	.3050	.1650	2.1600

**Note:**—RF indicates radiofrequency; T2W, T2-weighted.

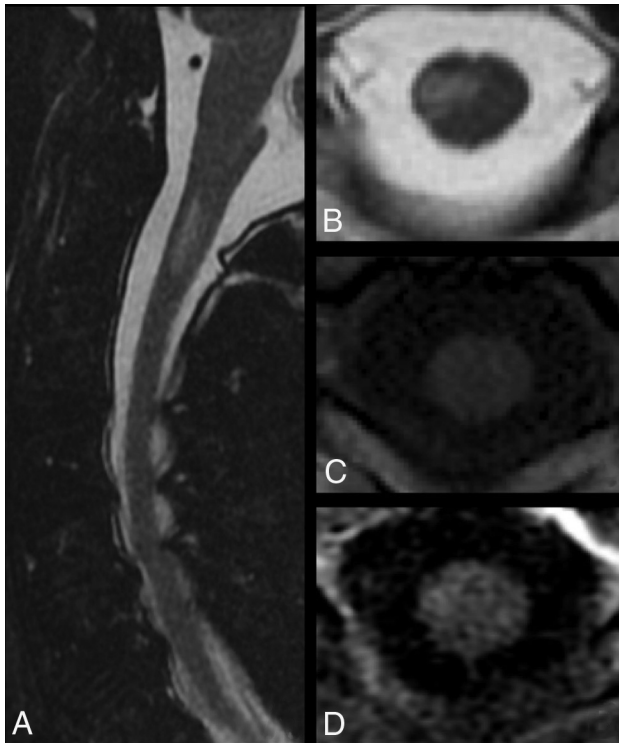


**FIG 3.** A, Sagittal T2-weighted image of the cervical spine for patient 6 shows hyperintensity in the anterior half of the cord at C1–C2. Axial T2-weighted image (B) shows hyperintensity in the right anterolateral quadrant. Axial T1-weighted (C) image with isointense signal in the lesion and a contrast-enhanced T1-weighted (D) image with no enhancement of the lesion.

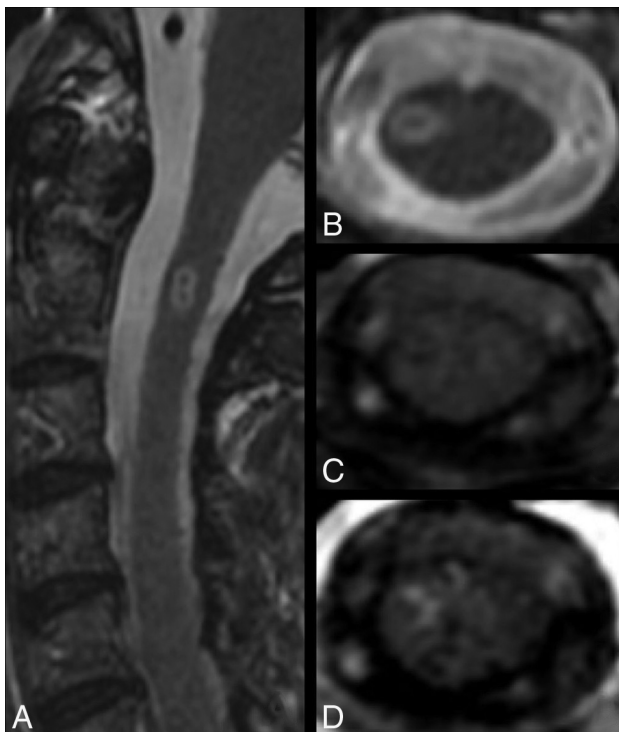


**FIG 4.** Sagittal T2-weighted image (A) and axial T2-weighted image (B) of the cervical spine of patient 4 show hyperintensity with central hypointensity at C1–C2. Axial T1-weighted (C) and contrast-enhanced T1-weighted (D) images show an isointense lesion with peripheral enhancement.

dorsolateral region of the ALQ (area =  $0.07 \pm 0.01 \text{ cm}^2$ , 66% of the anterolateral quadrant).

The number of pial penetrations correlated with the percentage of total cord area that was lesioned ( $r = 0.78$ ; 95% CI, 0.44–0.89;  $P = .008$ ) as well as the length of T2-weighted hyperintensity ( $r = 0.85$ ; 95% CI, 0.54–0.89;  $P = .002$ ). The number of radiofrequency ablations correlated with the percentage of lesion in the ALQ ( $r = 0.66$ ; 95% CI, 0.0–0.95;  $P = .04$ ) as well as the area of the lesion in the ventromedial region of the ALQ ( $r = 0.72$ ; 95% CI, 0.22–0.95;  $P = .02$ ).

#### **Clinical Correlations of Quantitative MR Imaging Data**

The percentage area of cord lesioned did not correlate with the change in VAS ( $r = -0.04$ ; 95% CI,  $-0.72$ – $0.75$ ;  $P = .92$ ), PSS ( $r = 0.18$ ; 95% CI,  $-0.63$ – $0.82$ ;  $P = .63$ ), or PIS ( $r = 0.38$ ; 95% CI,  $-0.44$ – $0.86$ ;  $P = .28$ ) scores at 7 days after the procedure.

The signal intensity in the lesions did not correlate with changes in the VAS ( $r = -0.28$ ; 95% CI,  $-0.77$ – $0.57$ ;  $P = .44$ ), PSS ( $r = -0.01$ ; 95% CI,  $-0.67$ – $0.72$ ;  $P = .97$ ), or PIS ( $r = -0.02$ ; 95% CI,  $-0.86$ – $0.67$ ;  $P = .96$ ) scores at postprocedure day 7.

Three patients had <20% of total cord area lesioned, and there was no significant difference for the change in VAS ( $5.7 \pm 1.5$  versus  $5.4 \pm 3.2$ ,  $P = .91$ ), PSS ( $4.3 \pm 0.87$  versus  $5.0 \pm 2.6$ ,  $P = .65$ ), and PIS ( $5.6 \pm 1.6$  versus  $6.9 \pm 2.1$ ,  $P = .39$ ) at 7 days postprocedure for these patients compared with those with >20% of total cord area lesioned.

#### **DISCUSSION**

We report one of the first clinical studies to describe MR imaging characteristics of the cordotomy lesion created by radiofrequency ablation. All lesions were hyperintense on T2-weighted imaging, and most lesions were isointense on T1-weighted imaging. Contrast enhancement was seen in 50% of the lesions. The area of the lesion correlated with the number of pial penetrations and radiofrequency ablations performed.

There are limited data on the evaluation of patients with poor outcomes after cordotomy. Inadequate lesioning and the presence of alternate pain pathways are reported to be responsible for poor outcomes after cordotomy.<sup>5</sup> MR imaging can define the anatomic location of the lesion, and scalar metrics of the lesion on T2-weighted imaging correlate with the number of radiofrequency ablations. Early changes visualized on MR imaging after cordotomy may result from edema, demyelination, and axonal injury created by radiofrequency lesioning.<sup>10</sup> Previous authors have reported similar T2-weighted hyperintensity and central hypointensity after radiofrequency ablation for intracranial targets<sup>11</sup> and after spinal cord ablation in nonhuman models.<sup>12</sup> The central hypointensity on T2-weighted imaging likely represents parenchymal injury from hemorrhagic coagulative necrosis adjacent to the radiofrequency electrode.<sup>13</sup> Prior studies have hypothesized isointense lesions on T1-weighted MR imaging, but we had 1 patient with a hyperintense lesion, which may represent acute-to-early subacute microhemorrhage within the lesion. The presence of contrast enhancement, which likely indicates a breach of the blood–spinal cord barrier, was seen in 5 of 9 patients (55.6%). Repair of the blood–spinal cord barrier may lead to reduced con-

trast enhancement of the lesion with time.<sup>11</sup> Although we found no statistically significant associations for contrast enhancement of the cordotomy lesion, larger studies are required to determine the impact of time and the number of lesions on contrast enhancement of the cordotomy lesion.

Prior studies have indicated that approximately 20% of the total cord area must be ablated for acceptable pain outcomes.<sup>14</sup> To further evaluate this finding, we measured the area of the cordotomy lesion on axial T2-weighted MR images. Most patients had >20% of the total cord area lesioned; however, there was no statistically significant correlation between lesion area and clinical outcome in our study. A larger lesion area may not represent adequate ablation of the spinothalamic tracts. This possibility highlights the importance of accurate localization of the target during the cordotomy procedure. Most lesions in the present study were in the dorsolateral region of the ALQ. This is in agreement with the histopathologic localization of pain pathways by Lahuerta et al,<sup>14</sup> though these authors suggested that more medially located lesions produce better pain relief. Radiofrequency lesions, however, have been shown to vary in size due to differences in microcirculation and tissue resistance.<sup>6,15</sup> In this study, we found that the number of pial penetrations and radiofrequency ablations was directly correlated with the area of the lesion. Pial penetrations were events in which the electrode was inserted into the cord but lesioning was not necessarily performed. Each pial penetration can create a small degree of trauma to the cord parenchyma and possibly edema as well, which may contribute to size of T2-weighted hyperintensity on postoperative imaging. These findings are important for surgeons and neurointerventionalists to consider when evaluating postoperative cordotomy MR images.

We found that the area and signal intensity of the lesion on T2-weighted imaging did not correlate with early clinical outcomes in our study. Although these results need to be verified in a larger patient population, one possible reason could be that early T2-weighted changes may not exclusively reflect neural ablation. Early postoperative imaging, however, can help visualize the location of the lesion and perhaps explain unsatisfactory pain outcomes at follow-up. Also, our protocol offers a practical time point for imaging because many of these patients are hospitalized for only 24 hours after the procedure. We did not perform subsequent follow-up MR imaging, though this could potentially improve our evaluation of the cordotomy lesion. It is possible that delayed imaging and the use of advanced MR imaging such as diffusion tensor imaging may help further investigate microstructural changes in the spinal cord after ablation.

This study is limited by the small number of patients and short-term clinical outcomes. Although we show that early postoperative MR imaging after percutaneous cordotomy is a feasible technique, it is important to keep scan times short because patients with intractable cancer pain may not be able to lie still for prolonged intervals. Overall, we present a description of the cordotomy lesion on early postoperative MR imaging in a prospective cohort and intend to further explore the utility of this technique in improving the accuracy of lesioning and predicting outcome.

## CONCLUSIONS

In this study, we characterize early MR imaging features after percutaneous cordotomy for intractable cancer pain. On early T2-weighted imaging, the lesions were hyperintense with a central hypointense focus. Quantitative MR imaging metrics of the cordotomy lesion correlate with the number of radiofrequency ablations; however, these metrics did not correlate with early clinical outcome. Delayed MR imaging and alternate MRI sequences such as diffusion tensor imaging may provide more accurate quantification of neural ablations.

Disclosures: Aditya Vedantam—RELATED: Grant: American Cancer Society,\* Comments: grant PEP-14-205-01. Kenneth R. Hess—UNRELATED: Travel/Accommodations/Meeting Expenses Unrelated to Activities Listed: Angiochem Inc., Comments: for presentation to the FDA. Patrick M. Dougherty—UNRELATED: Grant: National Cancer Institute.\* Ashwin Viswanathan—RELATED: Grant: American Cancer Society,\* Comments: Pilot Project in Palliative Care grant; Support for Travel to Meetings for the Study or Other Purposes: American Cancer Society, Comments: part of grant included travel to palliative care meeting.\* \*Money paid to the institution.

## REFERENCES

1. Kanpolat Y, Ugur HC, Ayten M, et al. **Computed tomography-guided percutaneous cordotomy for intractable pain in malignancy.** *Neurosurgery* 2009;64:ons187–93; discussion ons193–94 Medline
2. Harsh V, Viswanathan A. **Surgical/radiological interventions for cancer pain.** *Curr Pain Headache Rep* 2013;17:331 CrossRef Medline
3. Reddy GD, Okhuysen-Cawley R, Harsh V, et al. **Percutaneous CT-guided cordotomy for the treatment of pediatric cancer pain.** *J Neurosurg Pediatr* 2013;12:93–96 CrossRef Medline
4. Raslan AM. **Percutaneous computed tomography-guided radiofrequency ablation of upper spinal cord pain pathways for cancer-related pain.** *Neurosurgery* 2008;62:226–33; discussion 233–34 Medline
5. Mooij JJ, Bosch DA, Beks JW. **The cause of failure in high cervical percutaneous cordotomy: an analysis.** *Acta Neurochir (Wien)* 1984;72:1–14 CrossRef Medline
6. Aronow S. **The use of radio-frequency power in making lesions in the brain.** *J Neurosurg* 1960;17:431–38 CrossRef Medline
7. Cleeland CS, Ryan KM. **Pain assessment: global use of the Brief Pain Inventory.** *Ann Acad Med Singapore* 1994;23:129–38 Medline
8. Burton AW, Chai T, Smith LS. **Cancer pain assessment.** *Curr Opin Support Palliat Care* 2014;8:112–16 CrossRef Medline
9. Cleeland CS. **The measurement of pain from metastatic bone disease: capturing the patient's experience.** *Clin Cancer Res* 2006;12:6236s–42s CrossRef Medline
10. Vatansever D, Tekin I, Tuglu I, et al. **A comparison of the neuroablative effects of conventional and pulsed radiofrequency techniques.** *Clin J Pain* 2008;24:717–24 CrossRef Medline
11. De Salles AA, Brekhus SD, De Souza EC, et al. **Early postoperative appearance of radiofrequency lesions on magnetic resonance imaging.** *Neurosurgery* 1995;36:932–36; discussion 936–37 CrossRef Medline
12. Haghghi SS, Perez-Espejo MA, Rodriguez F, et al. **Radiofrequency as a lesioning model in experimental spinal cord injury.** *Spinal Cord* 1996;34:214–19 CrossRef Medline
13. Tomlinson FH, Jack CR Jr, Kelly PJ. **Sequential magnetic resonance imaging following stereotactic radiofrequency ventralis lateralis thalamotomy.** *J Neurosurg* 1991;74:579–84 CrossRef Medline
14. Lahuerta J, Bowsher D, Lipton S, et al. **Percutaneous cervical cordotomy: a review of 181 operations on 146 patients with a study on the location of "pain fibers" in the C-2 spinal cord segment of 29 cases.** *J Neurosurg* 1994;80:975–85 CrossRef Medline
15. Vonbonin G, Alberts WW, Wright EW Jr, et al. **Radiofrequency brain lesions. size as a function of physical parameters.** *Arch Neurol* 1965;12:25–29 CrossRef Medline